Dendritic D-type potassium currents inhibit the spike afterdepolarization in rat hippocampal CA1 pyramidal neurons

Alexia E. Metz[1,2], Nelson Spruston[2] and Marco Martina[1]

[1]*Department of Physiology, Feinberg School of Medicine, Chicago, IL 60611, USA*
[2]*Department of Neurobiology and Physiology, Northwestern University, Evanston, IL 60208, USA*

In CA1 pyramidal neurons, burst firing is correlated with hippocampally dependent behaviours and modulation of synaptic strength. One of the mechanisms underlying burst firing in these cells is the afterdepolarization (ADP) that follows each action potential. Previous work has shown that the ADP results from the interaction of several depolarizing and hyperpolarizing conductances located in the soma and the dendrites. By using patch-clamp recordings from acute rat hippocampal slices we show that D-type potassium current modulates the size of the ADP and the bursting of CA1 pyramidal neurons. Sensitivity to α-dendrotoxin suggests that Kv1-containing potassium channels mediate this current. Dual somato-dendritic recording, outside-out dendritic recordings, and focal application of dendrotoxin together indicate that the channels mediating this current are located in the apical dendrites. Thus, our data present evidence for a dendritic segregation of Kv1-like channels in CA1 pyramidal neurons and identify a novel action for these channels, showing that they inhibit action potential bursting by restricting the size of the ADP.

(Resubmitted 19 December 2006; accepted after revision 20 February 2007; first published online 22 February 2007)
Corresponding author M. Martina: Department of Physiology, Northwestern University Feinberg School of Medicine, 303 E. Chicago Avenue, Chicago, IL 60611, USA. Email: m-martina@northwestern.edu

Although intrinsically quiescent, ∼20% of CA1 pyramidal neurons demonstrate action potential bursting upon sustained input (Azouz *et al.* 1996; Jensen *et al.* 1996; Staff *et al.* 2000; Su *et al.* 2001; Metz *et al.* 2005). This firing mode is thought to be important for the function of the hippocampus in learning and memory. For example, action potential bursting in CA1 pyramidal neurons has been correlated with hippocampally dependent learning tasks (Ranck, 1973; O'Keefe, 1976; Suzuki & Smith, 1985*a*,*b*; Muller *et al.* 1987; Otto *et al.* 1991; Harris *et al.* 2001) and enhancement of synaptic strength (Thomas *et al.* 1998; Pike *et al.* 1999; Fortin & Bronzino, 2001). Because of the importance of CA1 pyramidal neuron action potential bursting in the function of the hippocampus, the intrinsic properties that confer the ability to burst have been the subject of intense investigation. The picture that has emerged is that the afterdepolarization (ADP), a depolarizing envelope that follows the fast phase of action potential repolarization (Schwartzkroin, 1975; Storm, 1987), is a robust mechanism for driving bursting (Azouz *et al.* 1996; Jensen *et al.* 1996; Magee & Carruth, 1999; Metz *et al.* 2005). Persistent sodium current has been shown to contribute to the ADP, especially when the external calcium concentration is low (Azouz *et al.* 1996; Yue *et al.* 2005; Chen *et al.* 2005). In addition, we recently demonstrated that under physiological calcium conditions, somatic R-type calcium current contributes to the ADP (Metz *et al.* 2005). Although the persistent sodium and the R-type calcium current that contribute to the ADP have been shown to originate mainly from the somatic compartment (Chen *et al.* 2005; Metz *et al.* 2005), both of these currents are also present in the apical dendrite of CA1 pyramidal neurons (Christie *et al.* 1995; Magee & Johnston, 1995*a*,*b*; Magee *et al.* 1995; Lipowsky *et al.* 1996; Isomura *et al.* 2002; Yasuda *et al.* 2003) where they can be activated by backpropagated action potentials. In fact, activation of inward voltage-gated currents by back-propagated action potentials has been shown to enhance the ADP and bursting in other pyramidal neurons (Mainen & Sejnowski, 1996; Williams & Stuart, 1999; Lemon & Turner, 2000).

The dendritic contribution to the ADP is not only determined by inward currents but is also shaped by dendritic potassium currents. Magee & Carruth (1999) showed that application of the potassium channel antagonist 4-aminopyridine (4-AP) to the dendrites – but not to the soma – promotes bursting through potentiation

This paper has online supplemental material.

DOI: 10.1113/jphysiol.2006.127068

of the ADP, and concluded that the effect was mediated by the block of A-type current. However, 4-AP also potently reduces the relatively non-inactivating, D-type potassium current (Storm, 1988; Grissmer *et al.* 1994), which is also present in CA1 pyramidal neuron dendrites (Hoffman *et al.* 1997; Chen & Johnston, 2004).

D-type potassium current was first described in CA1 pyramidal neurons and named for the delay it imposes on action potential firing in response to long current injections (Storm, 1988); however, neither the molecular determinants of D-type current, nor its specific role in modulating the ADP and bursting have been investigated in these neurons. Channels belonging to the Kv1 family, which are blocked by α-dendrotoxin (DTX; Storm, 1990; Grissmer *et al.* 1994), are potential candidates for mediating this current as they have been shown to enhance excitability and bursting in CA3 and neocortical pyramidal neurons (Bekkers & Delaney, 2001; Lopantsev *et al.* 2003). In CA1 pyramidal cells, DTX enhances initiation of dendritic spiking (Golding *et al.* 1999), another mechanism for producing bursting. The location of Kv1 channels in CA1 pyramidal cells is still unresolved. There is very little DTX-sensitive current in somatic nucleated patches from CA1 pyramidal cells (Martina *et al.* 1998), yet these cells express several Kv1 family mRNAs (Sheng *et al.* 1994; Martina *et al.* 1998). Moreover, the stratum radiatum – through which the apical dendrites of CA1 pyramidal cells extend – is immunopositive for Kv1.2 (Sheng *et al.* 1994), suggesting localization of these channels in the apical dendrites where they may be aptly situated to inhibit the ADP.

In this study we tested the joint hypotheses that inward voltage-gated currents in the apical dendritic tree, activated by the backpropagated action potential, have the capacity to contribute to the production of the ADP, yet the magnitude of the contribution is restricted by dendritic DTX-sensitive, D-type potassium currents. We used simultaneous somatic and dendritic current-clamp recordings, excised dendritic patches, and selective pharmacology to test these hypotheses. Using a novel recording configuration to functionally remove the contribution of the dendrite, we show that under control conditions the dendritic current provides a small contribution to the ADP, but when D-type currents are blocked the dendritic contribution is more than doubled. Focal application of DTX and voltage-clamp recordings in dendritic outside-out patches reveal that the D-type current is localized to the apical dendrite.

Methods

All animal procedures were approved by the Northwestern University Animal Care and Use Committee.

Tissue preparation

Male Wistar rats, 14–26 days old, were used for the preparation of transverse hippocampal slices following standard procedures. Animals were deeply anaesthetized with halothane or isofluorane inhalation ($\sim$200 μl to 1 l container, vaporized) and killed by decapitation. The brain was removed and sliced in ice-cold artificial cerebral spinal fluid (ACSF; see 'Solutions and drugs' section). Slices were transferred to a suspended mesh within a chamber containing sucrose solution (see below), incubated at 35°C for 15–20 min, and subsequently stored at room temperature. For recording, individual slices were transferred to a small chamber continuously perfused with ACSF at 1–3 ml min^{-1}, and visualized with an upright, fixed-stage microscope (Axioscop, Zeiss) using differential interference contrast infrared video-microscopy at $\times$60–160 magnification.

Whole-cell recordings

Whole-cell recordings were performed at 33–35°C using either a BVC-700 amplifier (Dagan Products, Minneapolis, MN, USA) or an Axopatch 200B (Axon Instruments, Union City, CA, USA) employing series resistance and capacitance compensation. Patch electrodes (3–6 MΩ) were made from thick-walled borosilicate glass (Garner Glass, Claremont, CA, USA or Hilgenberg, Malsfeld, Germany) and filled with K-gluconate internal solution. Only cells with membrane potentials negative to $-$55 mV were used for experiments. Membrane potential was maintained at $-$67 mV with somatic DC current injection as needed (0 to $-$150 pA). Data were filtered at 10 kHz and sampled at 100 kHz.

For electronic-excision experiments, the voltage output of the somatic amplifier in current-clamp mode was appropriately scaled and used as the voltage command to the dendritic amplifier by passing it through a pre-amplifier (Warner Instruments, Hamden, CT, USA). Only recordings in which series resistance was less than 15 MΩ, stable, and at least 65% compensated (with 20 μs or less lag) were used for analysis.

Recordings were made in the presence of kynurenic acid (2 mM) and picrotoxin (100 μM) to block fast synaptic excitatory and inhibitory transmission, respectively.

Outside-out recordings

Voltage-clamp recordings were performed in outside-out patches pulled from the apical dendrites of CA1 pyramidal cells 25–60 μm from the soma. Recordings were done at room temperature (22–24°C) using a patch-clamp amplifier (Axopatch 200B, Axon Instruments). Data were filtered at 2 kHz and sampled at 20 kHz. Patch pipettes of 2.5–4 MΩ contained KCl internal solution. Pipettes

were wrapped in Parafilm (Pechiney, Chicago, IL, USA) to minimize capacitive transients, the remainders of which were cancelled using the fast compensation circuitry of the amplifier. The whole-cell configuration was first obtained and the pyramidal identity of cells was confirmed by presence of sag in the membrane potential in response to a hyperpolarizing current injection and spike frequency adaptation. In patch recordings, leakage and capacitive currents were subtracted using $P/-4$ protocols. Stimuli were repeated 5–15 times and results were averaged.

Solutions and drugs

Unless otherwise indicated, chemicals were obtained from Sigma (St Louis, MO, USA). ACSF contained (mM): 125 NaCl, 25 $NaHCO_3$, 2.5 KCl, 1.25 NaH_2PO_4, 25 glucose, 2 $CaCl_2$ and 1 $MgCl_2$. Sucrose solution contained (mM): 87 NaCl, 25 $NaHCO_3$, 25 glucose, 75 sucrose, 2.5 KCl, 1.25 NaH_2PO_4, 0.5 $CaCl_2$, and 7 $MgCl_2$. ACSF and sucrose solutions were bubbled with a 95% O_2 and 5% CO_2 gas mixture. K-gluconate internal solution contained (mM): 140 K-gluconate, 10 NaCl, 5 EGTA, 10 Hepes, 2 Mg-ATP, 0.3 Na-GTP. The KCl internal solution contained (mM): 140 KCl, 10 NaCl, 2 $MgCl_2$, 2 Na_2-ATP, 0.3 Na-GTP, 10 EGTA, 10 Hepes. We used K-gluconate solution because, using this internal solution, the ADP amplitude has been shown to remain very stable for at least 45 min (Kaczorowski *et al.* 2007), exceeding the duration of our recordings. In some recordings, 5 mM KF was substituted for 5 mM KCl. All internal solutions were adjusted to pH 7.3 (with KOH) and contained 0.1% biocytin for later histological staining. Voltage-clamp recordings were performed in Hepes-buffered ACSF containing (mM): 138 NaCl, 2.5 KCl, 10 Hepes, 25 glucose, 2 $CaCl_2$, and 1 $MgCl_2$ (pH 7.3 with NaOH). DTX (Alomone Laboratories, Jerusalem, Israel) was always co-applied with 0.05% BSA. For bath application experiments, DTX was included in the ACSF. For outside-out patch recordings and local application, DTX was in solution with Hepes-buffered ACSF. For outside-out recordings, drugs were applied to the patches by using a multibarrel system consisting of four glass capillaries (1.5 mm i.d.) glued together and connected to a syringe pump (WPI, Sarasota, FL, USA). The patch-pipette carrying the patch was inserted into each of the pipes, which contained Hepes-buffered ACSF (pH 7.4) plus the drugs of interest.

Local drug application in slices was achieved by applying light positive pressure to the back of a small-bore patch pipette. The location of the cloud of perfusate was confirmed, in a subset of recordings, via two-photon laser scanning fluorescent microscopy (see Fig. 1 in online Supplemental material); 200 μM Fluo4 and 10 μM Alexa 594 (Molecular Probes, Carlsbad, CA, USA) were included in the intracellular solution and 40 μM Alexa 594 was included in the perfusion pipette. The dyes were excited by laser scanning at 806 nm. Emission was detected with separate, tuned photomultiplier tubes. The cloud of fluorescence was limited to the applied region and washed away in the direction of the apical dendrites and above the plane of the cell. Pharmacological effects were measured at steady state. When DTX was bath applied to the slices, it could not be washed out, but reversibility was obtained in outside-out patches and with focal application.

Data acquisition and analysis

Data were transferred to a computer during experiments, by either an ITC-18 digital-analog converter (Instrutech, Port Washington, NY, USA) or a Digidata 1322A (Axon Instruments). Igor Pro (Wavemetrics, Lake Oswego, OR, USA) and pCLAMP (Axon Instruments) software were used for acquisition and analysis. Statistical tests were performed using Excel software (Microsoft, Redmond, WA, USA). All results are reported as mean ± S.E.M.; error bars in the figures also represent S.E.M. Statistical significance was assessed by paired two-tailed t tests, unless otherwise indicated.

Action potentials were evoked by brief current injections with amplitudes just above threshold for reliable firing. The ADP is reported as the average membrane potential, relative to the resting membrane potential (for 10 ms before the spike), in the first 10 ms following the fast phase of action potential repolarization (the point at which the change in voltage with time reached a minimum as detected in the derivative of the waveform). Traces used for analysis were from 10 to 15 averaged recordings. Input resistance was determined from the slope of the steady-state voltage *versus* current plot that resulted from giving 600 ms current injections ranging from −150 to 50 pA. The concentration–response curve of the enhancement of the ADP by DTX was determined by fitting the data with a Hill equation in the form of

$$\mathrm{ADP_{DTX}}/\mathrm{ADP_{control}} = 1 + (1/(1 + (K_d/[\mathrm{DTX}])^n)),$$

where $\mathrm{ADP_{DTX}}/\mathrm{ADP_{control}}$ is the amplitude of the ADP in DTX relative to control, [DTX] is the concentration of DTX, K_d is the half-maximal concentration, and n is the Hill coefficient.

To construct activation curves, chord conductance (G) was calculated from the peak current within the first 25 ms of the pulse, assuming ohmic behaviour and a reversal potential of −105 mV – the equilibrium potential predicted by the Nernst equation for our experimental conditions. Activation curves were fitted with a Boltzmann function with the form

$$f(V) = 1/(1 + \exp(-(V - V_{1/2})/k),$$

where V is the membrane potential, $V_{1/2}$ is the voltage at which the activation is half-maximal, and k is the slope factor. The results reported in the text reflect the averages of the fits of data from individual patches.

In order to compare with literature values for heterologously expressed Kv1 channels, the time course of DTX-sensitive current activation was determined by fitting currents with an exponential equation:

$$f(t) = I_{\max}(1 - e^{(-t/\tau)}),$$

where $I_{\max}$ is the peak current and t is time, yielding a time constant (τ); therefore, we also used this fit for the composite potassium current and DTX-resistant current.

Results

Apical dendrite contribution to the ADP

To study the dendritic contribution to the ADP, we performed simultaneous current-clamp recordings from soma and apical dendrites. In order to observe the net effect of the entire apical dendritic tree on somatic ADPs, dendrites were patched proximal to the first large branch point; the membrane potential was very similar at the two locations, having a value of -62.4 ± 0.9 mV at the soma and -62.7 ± 1 mV at the dendrite ($n = 19$). Single action potentials were evoked by suprathreshold 2 ms current injections at the soma. The resulting ADPs measured in the dendrite were consistently larger than their somatic counterparts (13.5 ± 0.6 mV in the soma, *versus* 14.2 ± 0.7 mV in the dendrite, $n = 23$, $P < 0.01$, Fig. 1). Comparing the membrane potentials of the two recording sites by point-by-point subtraction of the dendritic from the somatic trace revealed that the dendrite is depolarized relative to the soma, beginning during the fast phase of action potential repolarization and throughout the ADP, with the maximum difference appearing ~1 ms after the peak of the action potential (Fig. 1*B* and *D*).

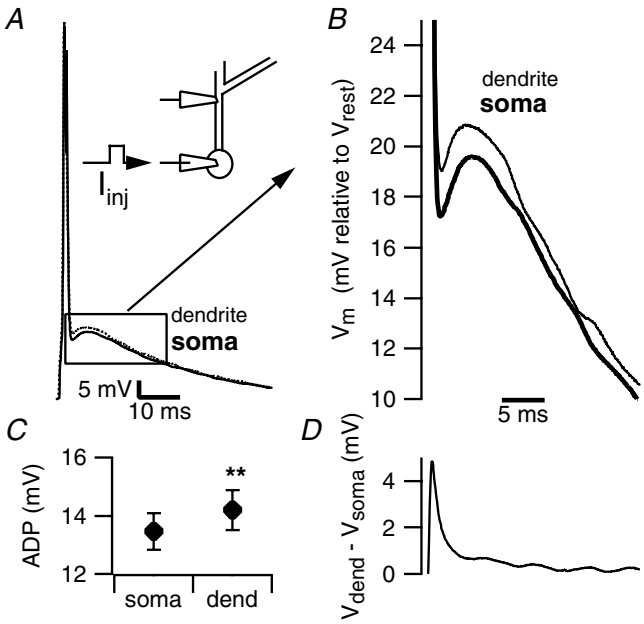

Figure 1. The afterdepolarization in the apical dendrite is larger than in the soma
A, simultaneous recording from the soma and apical dendrite of a CA1 pyramidal cell. Action potentials were evoked with current injection through the somatic pipette. The inset schematic diagram depicts the recording configuration for these experiments. *B*, the same recordings as in *A* are shown on a larger time scale. At this resolution it is clear that the dendritic ADP (thin trace) is larger than the somatic ADP (thick trace). *C*, plot summarizing the average size of somatic and dendritic ADP in 23 dual recordings. $^{**}P < 0.01$. *D*, for each paired recording, the somatic trace was digitally subtracted from the dendritic trace to reveal the time course of membrane potential differences. This trace is the population average of the resultant subtractions ($n = 23$). Free *x*-axis scale bar applies to *B* and *D*.

The membrane potential gradient between the dendrite and the soma generates a driving force for a flow of depolarizing current to the soma, which underlies the dendritic contribution to the ADP. Removing this driving force, then, should reduce the amplitude of the ADP. To accomplish this we performed simultaneous somatic and dendritic recordings, and the two amplifiers were connected so that the output of one could be used as the input of the other. At the beginning of the experiment (Fig. 2*A*, top) both the somatic and the dendritic pipettes were in current-clamp mode. Subsequently, the dendritic amplifier was switched to voltage-clamp mode (Fig. 2*A*, bottom) and its input signal consisted of the output (scaled to obtain a command voltage of the same amplitude) of the somatic amplifier. This eliminated, in real time, any difference in membrane potential between the two sites, producing a virtual 'electronic excision' of the dendrite. Electronic excision of the dendrite resulted in an average $10.7 \pm 2.1\%$ reduction in the size of the somatic ADP (the amplitude of the ADP measured at the somatic location was 13.9 ± 0.7 mV in the standard configuration *versus* 12.4 ± 0.8 with electronic excision, $n = 18$, $P < 0.01$, Fig. 2*C*). Control experiments, in which the second pipette was also positioned on the soma, were performed in order to rule out artifacts due to imperfect voltage clamp. In these experiments no change was detected in the size of the ADP (9.4 ± 1.2 mV in standard configuration *versus* 9.9 ± 1.4 mV with electronic excision, $n = 3$, $P > 0.05$, data not shown).

DTX-sensitive current, the ADP and bursting

While consistent, the effect of electronic excision was relatively small (the reduction in the size of ADP was ~1.5 mV). The apical dendrites of CA1 pyramidal neurons are rich with voltage-gated inward currents (Magee &

Johnston, 1995*a*) which, when activated by the back-propagating action potential, could contribute to the ADP. This suggests that other conductances may act to actively dampen the dendritic contribution to the ADP. Several types of potassium channels are differentially located in CA1 pyramidal neuron dendrites where they may serve such a role. M-type potassium currents in the proximal apical dendrite can do so (Yue & Yaari, 2004, 2006). Magee & Carruth (1999) demonstrated that 4-AP-sensitive, fast-inactivating dendritic A-type potassium current also provides such a restriction. D-type potassium current, which is also blocked by 4-AP, is another candidate for this action. To test this hypothesis, we used DTX, a selective blocker of Kv1-mediated D-type current. Bath application of 2 μM DTX resulted in a $38.6 \pm 4.5\%$ increase in the size of the ADP (14.8 ± 0.6 mV in control *versus* 20.5 ± 1 mV in DTX, measured at the soma, $n = 20$, $P < 0.01$, Fig. 3*A* and *D*). This was accompanied by a trend toward membrane depolarization as evidenced by a slight increase in holding current required to maintain a membrane potential of -67 mV (-37.1 ± 12.5 pA *versus* -46 ± 13.7 pA, $n = 19$, $P = 0.07$ Fig. 3*B*) and by an increase in input resistance (117 ± 7 MΩ in DTX *versus* 103 ± 6 MΩ in control, $n = 19$, $P < 0.01$, Fig. 3*C*), both indicating that the toxin blocked a conductance active at rest. In keeping with an action on Kv1 channels, the effect of DTX on the ADP was concentration dependent, with a half-maximal effect at ~5 nM, a concentration similar to that causing half-maximal block of Kv1.1 and Kv1.2 channels expressed in heterologous systems (Grissmer *et al.* 1994).

The enhancement of the ADP by DTX resulted in an increased propensity for action potential bursting in response to both simulated synaptic currents and sustained current injections. A simulated excitatory post-synaptic current (sEPSC) was injected in the soma during the ADP (Fig. 4*A*, lower panel), and its amplitude was increased until it evoked a second action potential. DTX decreased the amplitude of the sEPSC required to evoke the second spike (Fig. 4*B*); control measurements showed that in control conditions the amplitude of the ADP was unchanged during the same time span (not shown; see also Kaczorowski *et al.* 2007). To quantify this effect, we used the burst current index, a measure of the propensity to burst in response to such stimuli (Metz *et al.* 2005). In this index, the amplitude of the smallest sEPSC that evokes a second spike is expressed relative to the amplitude of the first 2 ms, suprathreshold current injection (which was unaffected: 387 ± 32 pA in control, 409 ± 38 in DTX, $n = 19$, $P > 0.05$). DTX reduced the burst current index

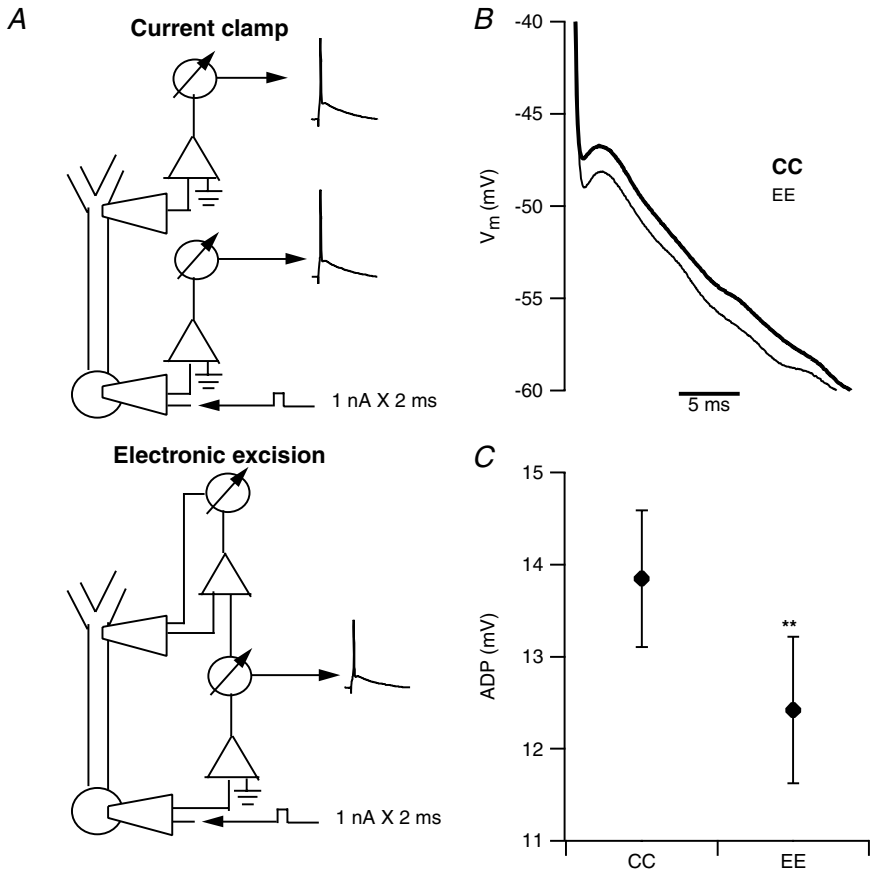

Figure 2. Electronic excision of the dendrite reduces the somatic afterdepolarization
A, top schematic diagram depicts the typical configuration for simultaneous current-clamp recordings (CC) from soma and dendrite. The lower schematic diagram shows the configuration for electronic excision of the dendrite (EE) in which the voltage signal recorded via the somatic pipette is used as the voltage command for the dendritic amplifier in voltage-clamp mode. This configuration eliminates, in real time, any membrane potential difference between the dendritic and the somatic pipette resulting in a functional excision of the dendrite. *B*, traces from a representative example showing that electronic excision of the dendrite reduced the size of the ADP recorded at the soma. *C*, plot showing the average effect of electronic excision of the dendrite on the ADP recorded at the soma in 18 different pyramidal neurons. The excision significantly (**$P < 0.01$) decreased the amplitude of the somatic ADP.

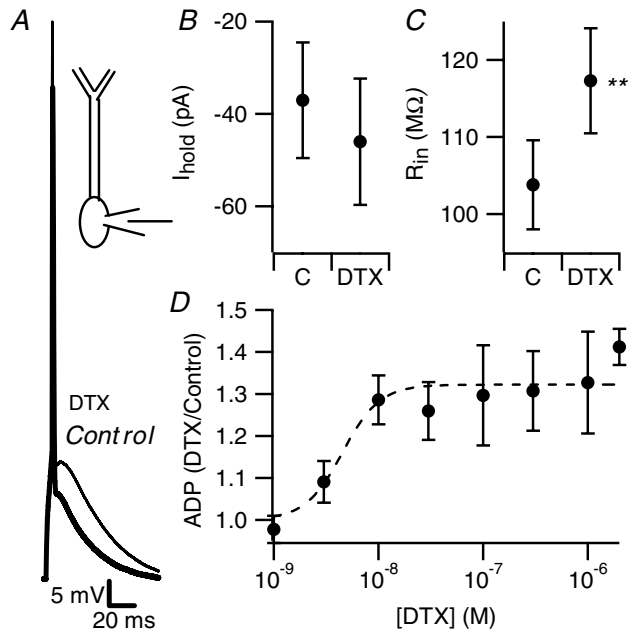

Figure 3. Dendrotoxin enhances the somatic afterdepolarization
A, bath-applied DTX enhanced the ADP. Voltage traces, recorded at the soma, in control conditions (thick trace) and in the presence of bath-applied dendrotoxin (2 μM, thinner trace), are shown superimposed. *B*, in the presence of 2 μM DTX, slightly more holding current was required to keep cells at –67 mV ($n = 19$, $P = 0.07$). *C*, in the same neurons, DTX increased input resistance. $^{**}P < 0.01$. *D*, DTX enhanced the ADP in a dose-dependent manner. The toxin concentration that caused half-maximal effect was determined by fitting the concentration—response curve with a Hill equation, constraining the Hill coefficient to 1. The best fit yielded a half-maximal concentration of 4.5 nM.

from 0.75 ± 0.04 to 0.46 ± 0.8 ($n = 19$, $P < 0.01$, Fig. 4*B*). The ADP following the second action potential was essentially the same size as the ADP of a single spike (14.8 ± 0.6 mV after a single spike, 15.3 ± 5 mV after an evoked burst, $P > 0.05$), and was similarly affected by DTX ($+30.8 \pm 5.5\%$, $n = 20$, $P < 0.05$, data not shown).

In some cells DTX also caused a just suprathreshold, 600 ms current injection to evoke a burst instead of a single spike at the beginning of the response (Fig. 4*C*). The percentage of cells that demonstrated action potential bursting in response to a 600 ms-long current injections increased from 20% to 45% (Fig. 4*D*). In order to quantify bursting, we calculated the interspike interval ratio (ISI ratio) in which the shortest ISI in a cell is divided by the average ISI in the same cell. This is based on our previous results (Metz *et al.* 2005), showing that cells with an ISI ratio of less than 0.1 represent a distinct subpopulation of CA1 pyramidal neurons, and therefore that bursting represents a specific firing phenotype and not merely the extreme of a continuous range.

Localization and characteristics of DTX-sensitive currents

To this point, DTX was bath applied in order to maximize its effect. To test whether DTX-sensitive K^+ channels are localized in the dendrites, as suggested by Sheng *et al.* (1994) and, very recently, by Raab-Graham *et al.* (2006), we next used focal application (Supplemental Fig. 1) of 500 nM DTX in three cellular regions: the

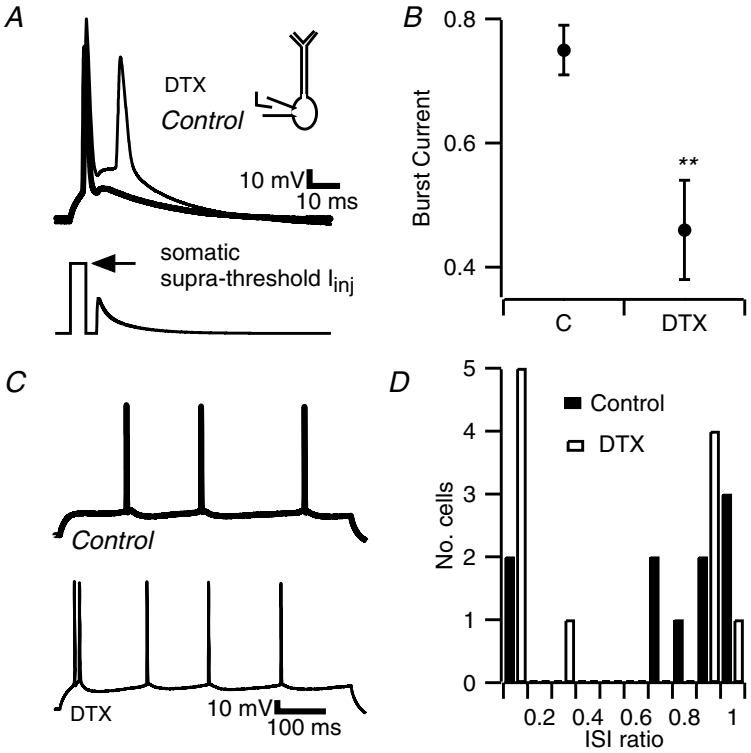

Figure 4. Dendrotoxin enhances bursting in CA1 pyramidal cells
A, current clamp recording obtained from the soma of a pyramidal cell. A simulated EPSC was injected at the soma 3 ms after the offset of the square pulse that elicited the first spike. DTX (2 μM, bath applied, thin trace), enhanced the ADP, allowing the EPSP (subthreshold in control condition, thick trace) to evoke a second spike. *B*, the minimum amplitude of the sEPSC that evoked a second spike was quantified relative to the size of the first, suprathreshold 2 ms current injection, and termed the burst current. DTX reduced the burst current ($n = 19$, $^{**}P < 0.01$). *C*, application of DTX caused bursting in response to sustained somatic current injection (600 ms). *D*, bursting was defined as responses to 600 ms current injection where the shortest interspike interval (ISI) was less than one-tenth of the average ISI (ISI ratio). DTX increased the percentage of bursting cells from 20% to 45%.

soma, the proximal apical dendrite (50–200 μm from the soma), and the distal apical dendrite (250 μm and beyond). Only application to the proximal dendrite (Fig. 5*A*) resulted in a significant enhancement of the ADP ($+1.0 \pm 0.5$ mV, $n = 17$, $P < 0.05$), although a trend was observable also for applications at larger distance ($+0.5 \pm 0.4$ mV $n = 13$, $P > 0.05$, Fig. 5*B*). While the lack of a significant effect with application of DTX to the distal apical dendrite does not rule out the possibility that there are DTX-sensitive currents in the distal dendrites, it does suggest that channels expressed in the proximal dendrite exert particular control over the somatically recorded ADP. The effect of focal application of DTX to the proximal dendrites was rapid and reversible (Fig. 5*C*), supporting the notion that DTX exerts its action by block of Kv1 channels.

In order to ascertain the contribution of DTX-sensitive current to the total potassium current in this critical region of the dendrite, and to determine some of the characteristics of the current, we tested the effect of DTX on potassium currents in outside-out patches from the proximal dendrites of CA1 pyramidal neurons. DTX (500 nM) reduced the peak potassium current by $16.4 \pm 4.9\%$ (Fig. 6*A-C*, $n = 12$, $P < 0.01$). For further confirmation of the effect of DTX on a distinct channel type, we compared the voltage dependence of activation in two populations of patches: one recorded in control conditions and the other in the presence of DTX. The activation curve of the current shifted rightward in DTX compared to control conditions. The average voltage of half-maximal activation was -19.3 ± 7.3 mV in control and 1 ± 3.8 mV in DTX ($n = 4$ each, $P < 0.05$, Fig. 6*D*) indicating that the DTX-sensitive current activated at hyperpolarized potentials relative to the other potassium current components, similar to what has been described for Kv1 channels in medial nucleus of the trapezoid body (MNTB) neurons (Brew & Forsythe, 1995). The DTX-sensitive current also had a slower activation than the other dendritic potassium currents, in keeping with the properties described for Kv1 delayed rectifier channels (Stühmer *et al.* 1989). The time course of activation of the current (at +40 mV) was 2.48 ± 1 ms for the DTX-sensitive component, and 1.22 ± 0.2 ms and 1.1 ± 0.2 ms for the total current and DTX-resistant component, $n = 4$, 11 and 9, respectively, $P < 0.05$ by ANOVA, data not shown).

Electronic excision of the dendrite in DTX

We have shown that DTX-sensitive currents are present in the proximal region of the dendrite. Their block causes an enhancement of the ADP, suggesting that they are critical in regulating the dendritic contribution to the ADP. To test this prediction, we performed electronic excision experiments in the presence of bath-applied DTX (250 nM). In these experiments DTX enhanced the size of the ADP measured at the soma by 1.6 ± 0.7 mV. Subsequent dendritic excision reduced the amplitude of this enlarged ADP from 14.8 ± 1.8 mV to 11.8 ± 1.5 mV ($n = 6$, $P = 0.01$), an effect larger than that of electronic excision of the dendrite under control conditions: the ADP was reduced by $20.3 \pm 4.3\%$ in DTX compared to $10.7 \pm 2.1\%$ in control (Fig. 7*B*). Figure 7*C* also shows that the size of the ADP with electronic excision of the dendrite is approximately the same in both control and DTX, suggesting that the reduction of the ADP caused by electronic excision of the dendrite in the presence of DTX was larger because the block, by the toxin, of dendritic D-type potassium channels unmasks

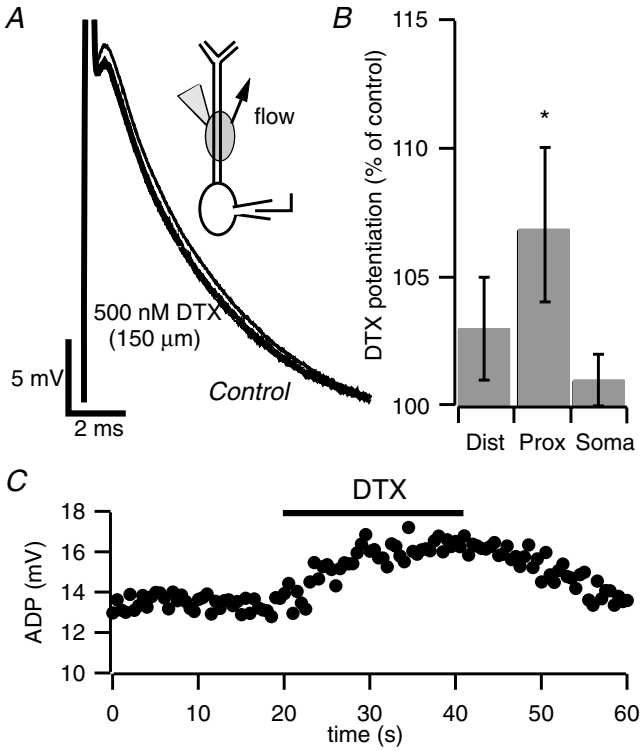

Figure 5. Local application of dendrotoxin to proximal apical dendrites enhances the afterdepolarization
A, current-clamp recording from the soma of a pyramidal neuron. Focal dendritic application of DTX at 150 μm from soma enhanced the ADP. The inset schematic diagram depicts local application of DTX to apical dendrites. The arrow represents the direction of the superfusion flow. The application pipette contained 500 nM DTX. *B*, bar chart depicting the potentiation of the somatic ADP by local application of DTX in three different cell compartments. Application of DTX to dendrites 250 μm and beyond (distal) resulted in a slight, non-significant, increase in the size of the ADP ($n = 13$, $P = 0.2$); application at 50—200 μm from the soma (proximal) caused an enhancement of the ADP ($n = 17$, $^*P < 0.05$); application to the soma did not affect the ADP ($n = 8$). *C*, time course of the enhancement of the somatic ADP by local application of DTX to the proximal apical dendrite. Action potentials were elicited by 2 ms current injections of 1.1 nA at a frequency of 0.03 Hz from a holding potential of –67 mV. Note the reversibility of the effect upon washout of the toxin.

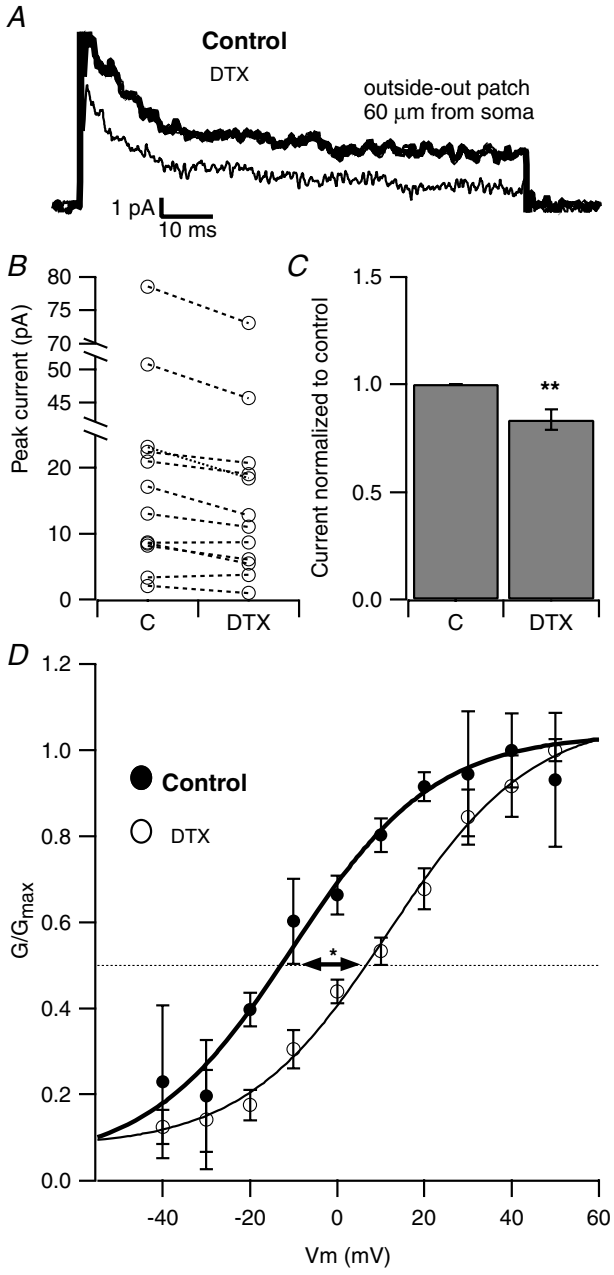

Figure 6. Apical dendrites express DTX-sensitive current
A, in a representative outside-out patch pulled from the apical dendrite of a CA1 pyramidal cell, DTX (500 nM) reduced the outward K^+ current. *B*, this plot shows the effect of DTX on individual dendritic outside-out patches. Each connected pair represents the potassium current amplitude obtained from the same patch in control condition and in the presence of DTX (500 nM). *C*, bar chart summarizing the effect of DTX on 12 patches from proximal apical dendrites (<100 μm from the soma). DTX caused a 16.4 ± 5.9% reduction of the total K^+ current. $^{**}P < 0.01$. *D*, DTX caused a rightward shift in the voltage dependence of activation of the dendritic potassium current. The data points, which represent population averages, were fitted with a Boltzmann equation. The resulting fit parameters were $V_{1/2} = -15.9$ mV, $k = 13.7$ in control, and $V_{1/2} = 6.8$ mV, $k = 18.0$ in DTX ($n = 4$ each, $^{*}P < 0.05$).

additional depolarizing current. These data support our hypothesis that DTX-sensitive, D-type potassium channels are localized in the apical dendrite and control the amplitude of the ADP of CA1 pyramidal neurons by limiting the contribution of the dendrite.

Discussion

Spatial distribution of currents regulating the ADP

The results of our experiments indicate that active apical dendrites enhance the somatic ADP and that dendritic, DTX-sensitive, D-type potassium channels limit this action.

Current flow from the dendrite has been shown to contribute to production of the ADP in several cell types (Mainen & Sejnowski, 1996; Williams & Stuart, 1999; Lemon & Turner, 2000; Dorion *et al.* 2003); however, it has been shown that in CA1 pyramidal neurons, a somatic current mediates the ADP (Metz *et al.* 2005; Yue *et al.* 2005; Golomb *et al.* 2006) except under conditions of potassium channel block, modulation, or inactivation

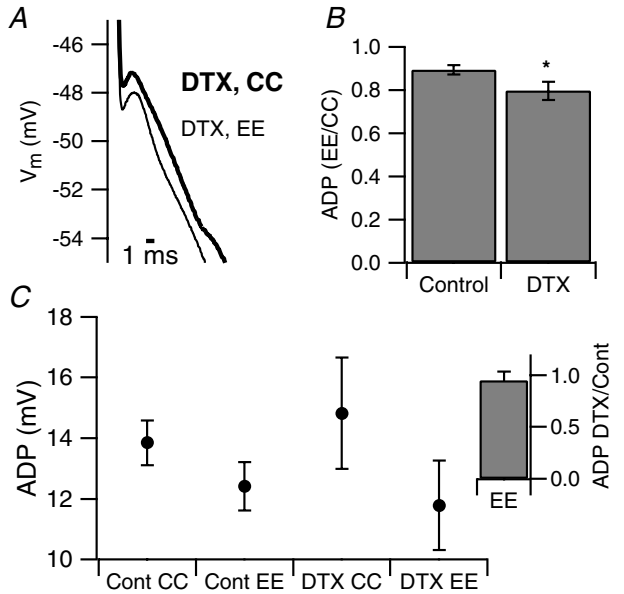

Figure 7. Electronic excision of the dendrite is more effective in dendrotoxin
A, representative example of somatic recordings showing the effect of electronic excision in the presence of 250 nM DTX. *B*, bar chart representing the size of the ADP recorded with dendritic excision normalized to the size of the ADP recorded in standard current clamp in control ACSF and in DTX. In DTX, electronic excision was more effective (−24.7 ± 4.5% ($n = 6$) compared to −10.7 ± 2.1% in control ($n = 18$) $^{*}P < 0.05$). *C*, population average of ADP size recorded in the standard current-clamp configuration (CC) and with electronic excision (EE) of the dendrite in the absence and in the presence of DTX ($n = 18$ and 6 for control and DTX, respectively). Inset, the size of the ADP during electronic excision is the same in the absence and in the presence of DTX.

(Magee & Carruth, 1999; Yue & Yaari, 2004, 2006; Yue *et al.* 2005). We show here that early in the ADP – beginning ~1 ms after the peak of the spike – the apical dendrites of CA1 pyramidal neurons are depolarized relative to the somata; as a consequence, current flow from the dendrite actively depolarizes the soma. The depolarization of the dendrite relative to the soma peaks during the fast phase of action potential repolarization and early in the ADP. Thus the dendritic contribution is synchronous with the fast, somatic, calcium tail current that underlies the ADP (Metz *et al.* 2005); this suggests that these two events are tuned to produce an ADP limited to a time window of just a few milliseconds. The remaining component of the ADP (>20 ms) may reflect near-passive decay of the active component of the ADP.

Potassium current in CA1 pyramidal neuron dendrites

Differential distribution of potassium channels in dendrites has previously been observed in several neuronal types. For instance, in the apical dendrites of CA1 pyramidal neurons, A-type current density increases with distance from the soma (Hoffman *et al.* 1997), while the I_{AHP} has been suggested to be mostly located in proximal dendrites (Sah & Bekkers, 1996). The ratio of inactivating to sustained current increases with distance also in Purkinje neuron dendrites (Martina *et al.* 2003) and, although to a lesser degree, in layer 5 pyramidal neurons (Bekkers, 2000; but see also Korngreen & Sakmann, 2000) because of an increasing density of fast inactivating K^+ current, just as in CA1 pyramidal neurons. Also G-protein-activated K^+ current density is enriched in neocortical pyramidal neuron apical dendrites (Takigawa & Alzheimer, 1999).

Several dendritic potassium currents have been shown to minimize the dendritic contribution to the ADP (Magee & Carruth, 1999; Yue & Yaari, 2004, 2006). Hints of the presence in CA1 pyramidal cell dendrites of DTX-sensitive, D-type potassium currents and their potential roles can be found in the literature. First, DTX-sensitive currents have been recorded in the dendrites of other cell types (Bekkers & Delaney, 2001; McKay *et al.* 2005; Guan *et al.* 2005). Second, there was faint staining for Kv1 protein and mRNA in the stratum radiatum of the CA1 pyramidal region in immunohistochemistry and in *in situ* hybridization studies (Sheng *et al.* 1994; Monaghan *et al.* 2001). Third, single-cell reverse transcription polymerase chain reaction experiments in CA1 pyramidal neurons detected mRNAs for several members of the Kv1 family, yet DTX-sensitive current is virtually absent from the soma of CA1 pyramidal neurons (Martina *et al.* 1998). Some of the staining results from Kv1 channels in Schaffer collateral terminals, which synapse onto the dendrites of the pyramidal neurons (Monaghan *et al.* 2001), but there is also clear staining for the Kv1-associated β_2 subunits in the soma and proximal dendrites of pyramidal neurons, suggesting the presence of Kv1-containing channels in these compartments (Rhodes *et al.* 1997). Fourth, very recent data show that Kv1 RNAs are detected in dendrites from hippocampal neurons (Raab-Graham *et al.* 2006). Finally, DTX also enhances dendritic calcium spikes, another mechanism for driving bursting in response to strong excitatory synaptic activation (Golding *et al.* 1999).

Our results confirm the presence of DTX-sensitive, D-type potassium current in the apical dendrites of CA1 pyramidal neurons. Furthermore, we show that DTX-sensitive channels directly influence the size of the ADP and regulate action potential firing mode. DTX-sensitive current inactivates considerably more slowly than A-type potassium current (Storm, 1990; Grissmer *et al.* 1994), so D-type potassium current would be able to continue to restrict the size of the ADP in the face of sustained depolarizing inputs as may happen during periods of high activity or seizures. In support of this, the ADP that followed the second spike in an evoked burst was enhanced by DTX to the same extent as the ADP following single spikes.

Local application of DTX to the proximal apical dendrite results in enhancement of the ADP, while distal application had a smaller, non-significant, effect. A possible interpretation of this result is that the density of DTX-sensitive channels is higher in the proximal than in the distal dendrite; however, another possibility is that DTX-sensitive channels are diffusely distributed throughout the dendrite but the increased depolarization resulting from local blockade in distal dendrites does not propagate to the soma because of the cable properties of the dendrites; the intervening, unblocked D-type K^+ channels in the proximal dendrites may further limit the effect of blocking distal channels alone. The proximal apical dendrite may therefore represent a critical region where the DTX-sensitive current regulates the contribution of the distal dendrite to the ADP. Bath application of DTX increases the ADP by a factor of 1.4 ± 0.5, compared to 1.1 ± 0.3 for proximal application. While this may result from a lack of saturation at the site of local application because of dilution, another possibility is that DTX-sensitive channels are also present in other compartments such as the distal apical dendrites, basal dendrites, or axon. The presence of DTX-sensitive channels beyond the proximal dendrites is also suggested by the results obtained in two cells where the ADP was first enhanced by local application of DTX (500 nM) to the proximal dendrite; subsequent bath application of DTX to the same neurons (at the same concentration) further increased the ADP (7%, in both cells, not shown).

Outside-out patch recordings show that ~16% of the total potassium current in the proximal dendrite is DTX

sensitive, a slightly higher proportion than is seen in neocortical pyramidal cell dendrites (Bekkers & Delaney, 2001), but similar to that in Purkinje neurons (McKay *et al.* 2005). The properties of the DTX-sensitive currents that we report here are similar to what has been described for native Kv1 channels in other preparations (Brau *et al.* 1990; Foehring & Surmeier, 1993; Brew & Forsyth, 1995; Nisenbaum *et al.* 1996; Southan & Robertson, 2000; Geiger & Jonas, 2000; Rothman & Manis, 2003; Guan *et al.* 2005). In our case, DTX caused a rightward shift in the current activation curve, suggesting that the blocked component is responsible for the current activated at more negative membrane potentials. The slow activation kinetics typical of the DTX-sensitive current make it ideal to contribute to shaping the membrane potential after a spike, while not contributing to the fast repolarization phase.

Functional role of dendritic D-type currents

KV1 channels have been shown to have several functions in determining the excitable properties of neurons. Genetic deletion resulting in loss of Kv1 protein results in seizure activity in CA3 pyramidal neurons by increasing axonal excitability (Lopantsev *et al.* 2003), whereas over-expression of Kv1 channels protect cells from entering depolarization block in response to sustained current injection (Kupper *et al.* 2002). Kv1 channels restrict release of neurotransmitter as in mossy fibres, the Calyx of Held, cerebellar basket cells, and thalamic inputs onto prefrontal cortical cells (Brau *et al.* 1990; Brew & Forsyth, 1995; Zhang *et al.* 1999; Southan & Robertson, 1998, 2000; Geiger *et al.* 2000; Lambe & Aghajanian, 2001; Lopantsev *et al.* 2003; Dodson *et al.* 2003). They serve to ensure faithful transmission across synapses by restricting postsynaptic excitability in neurons of the MNTB and Purkinje neurons (McKay *et al.* 2005; Brew & Forsyth, 1995; Gittelman & Tempel, 2006). In some cell types, such as neurons of the ventral cochlear nucleus (VCN) and MNTB, DTX-sensitive current serves to restrict overall excitability in response to sustained inputs (Dodson *et al.* 2002; Brew *et al.* 2003; Rothman *et al.* 2003).

Our finding that DTX-sensitive current inhibits action potential bursting by restricting the size of the ADP has implications for how these channels affect network function, as bursting has been theorized to enhance both neurotransmitter release (Malinow, 1994; Lisman, 1997; Izhikevich *et al.* 2003) and synaptic plasticity (Thomas *et al.* 1998; Pike *et al.* 1999). *In vivo* recordings in awake, behaving animals have demonstrated that CA1 pyramidal neurons fire in both regular spiking and bursting mode (Harris *et al.* 2001), and that bursting is associated with spatial tasks and memory formation (Ranck, 1973; Buzsáki, 1989). At the same time, increased action potential bursting in CA1 pyramidal cells is a prominent feature in animal models of epilepsy (Sanabria *et al.* 2001; Su *et al.* 2002). Hence it appears critical that the bursting be adaptively regulated in CA1 pyramidal cells. To this extent, multiple potassium currents serve to restrict the size of the ADP and subsequent bursting including A-type, M-type (Magee & Carruth, 1999; Yue & Yaari, 2004, 2006) and DTX-sensitive D-type currents. Interestingly, these channels are all targets of second messenger systems (Jonas & Kaczmarek, 1996; Hoffman & Johnston, 1998; Wu & Barish, 1999; Dong & White, 2003; Lambe & Aghajanian, 2001) allowing multiple possibilities for modulating action potential bursting.

References

Azouz R, Jensen MS & Yaari Y (1996). Ionic basis of spike after-depolarization and burst generation in adult hippocampal CA1 pyramidal cells. *J Physiol* **492**, 211–223.

Bekkers JM (2000). Distribution and activation of voltage-gated potassium channels in cell-attached and outside-out patches from large layer 5 cortical pyramidal neurons of the rat. *J Physiol* **525**, 611–620.

Bekkers JM & Delaney AJ (2001). Modulation of excitability by α-dendrotoxin-sensitive potassium channels in neocortical pyramidal neurons. *J Neurosci* **21**, 6553–6560.

Brau ME, Dreyer F & Jonas P (1990). A K^+ channel in *Xenopus* nerve fibres selectively blocked by bee and snake toxins: binding and voltage-clamp experiments. *J Physiol* **420**, 365–385.

Brew HM & Forsythe ID (1995). Two voltage-dependent K^+ conductances with complementary functions in postsynaptic integration at a central auditory synapse. *J Neurosci* **15**, 8011–8022.

Brew HM, Hallows JL & Tempel BL (2003). Hyperexcitability and reduced low threshold potassium currents in auditory neurons of mice lacking the channel subunit Kv1.1. *J Physiol* **548**, 1–20.

Buzsáki G (1989). Two-stage model of memory trace formation: a role for 'noisy' brain states. *Neuroscience* **31**, 551–570.

Chen X & Johnston D (2004). Properties of single voltage-dependent K^+ channels in dendrites of CA1 pyramidal neurons of rat hippocampus. *J Physiol* **559**, 187–203.

Chen S, Yue C & Yaari Y (2005). A transitional period of Ca^{2+}-dependent spike afterdepolarization and bursting in developing rat CA1 pyramidal cells. *J Physiol* **567**, 79–93.

Christie BR, Eliot LS, Ito K & Miyakawa H (1995). Different Ca^{2+} channels in soma and dendrites of hippocampal pyramidal neurons mediate spike-induced Ca^{2+} influx. *J Neurophysiol* **73**, 2553–2557.

Dodson PD, Barker MC & Forsythe ID (2002). Two heteromeric Kv1 potassium channels differentially regulate action potential firing. *J Neurosci* **22**, 6953–6961.

Dodson PD, Billups B, Rusznak Z, Szucs G, Barker MC & Forsythe D (2003). Presynaptic rat Kv1.2 channels suppress synaptic terminal hyperexcitability following action potential invasion. *J Physiol* **550**, 27–33.

Dong Y & White F (2003). Dopamine D1-class receptors selectively modulate a slowly inactivating potassium current in rat medial prefrontal cortex pyramidal neurons. *J Neurosci* **23**, 2686–2695.

Dorion B, Noonan L, Lemon N & Turner R (2003). Persistent Na^+ current modifies burst discharge by regulating condition backpropagation of dendritic spikes. *J Neurophysiol* **989**, 324–337.

Foehring RC & Surmeier DJ (1993). Voltage-gated potassium currents in acutely dissociated rat cortical neurons. *J Neurophysiol* **70**, 51–63.

Fortin DA & Bronzino JD (2001). The effect of interburst intervals on measures of hippocampal LTP in the freely moving adult male rat. *Exp Neurol* **170**, 371–374.

Geiger JRP & Jonas P (2000). Dynamic control of presynaptic Ca^{2+} inflow by fast-inactivating K^+ channels in hippocampal mossy fiber boutons. *Neuron* **28**, 927–939.

Gittelman JX & Tempel BL (2006). Kv1.1-containing channels are critical for temporal precision during spike initiation. *J Neurophysiol* **96**, 1203–1214.

Golding NL, Jung HY, Mickus T & Spruston N (1999). Dendritic calcium spike initiation and repolarization are controlled by distinct potassium channel subtypes in CA1 pyramidal neurons. *J Neurosci* **19**, 8789–8798.

Golomb D, Yue C & Yaari Y (2006). Contribution of persistent Na^+ current and M-type K^+ current to somatic bursting in CA1 pyramidal cells: combined experimental and modeling study. *J Neurophysiol* **96**, 1912–1926.

Grissmer S, Nguyen AN, Aiyar J, Hanson DC, Mather RJ, Gutman GA, Karmilowicz MJ, Auperin DD & Chandy GK (1994). Pharmacological characterization of five cloned voltage-gated K^+ channels, KV1.1, 1.2, 1.3, 1.5 and 3.1 stably expressed in mammalian cell lines. *Mol Pharm* **45**, 1227–1234.

Guan D, Lee JCF, Tkatch T, Surmeier DJ, Armstrong WE & Foehring RC (2005). Expression and biophysical properties of Kv1 channels in supragranular neocortical pyramidal neurons. *J Physiol* **571**, 371–389.

Harris KD, Hirase H, Leinekugel X, Henze DA & Buzsaki G (2001). Temporal interaction between single spikes and complex bursts in hippocampal pyramidal cells. *Neuron* **32**, 141–149.

Hoffman DA & Johnston D (1998). Downregulation of transient K^+ channels in dendrites of hippocampal CA1 pyramidal neurons by activation of PKA and PKC. *J Neurosci* **15**, 408–411.

Hoffman D, Magee JC, Costa CM & Johnston D (1997). K^+ channel regulation of signal propagation in dendrites of hippocampal pyramidal neurons. *Nature* **387**, 869–875.

Isomura Y, Fujiwara-Tsukamoto Y, Imanishi M, Nambu A & Takada M (2002). Distance-dependent Ni^{2+}-sensitivity of synaptic plasticity in apical dendrites of hippocampal CA1 pyramidal cells. *J Neurophysiol* **87**, 1169–1174.

Izhikevich EM, Desai NS, Walcott EC & Hoppensteadt FC (2003). Bursts as a unit of neural information: selective communication via resonance. *Trends Neurosci* **26**, 161–167.

Jensen MS, Azouz R & Yaari Y (1996). Spike after-depolarization and burst generation in adult rat hippocampal CA1 pyramidal cells. *J Physiol* **492**, 199–210.

Jonas EA & Kaczmarek LK (1996). Regulation of potassium channels by protein kinases. *Curr Opin Neurobiol* **6**, 318–323.

Kaczorowski CC, Disterhoft J & Spruston N (2007). Stability and plasticity of intrinsic membrane properties in hippocampal CA1 pyramidal neurons: effects of internal anions. *J Physiol* **578**, 799–818.

Korngreen A & Sakmann B (2000). Voltage-gated K^+ channels in layer 5 neocortical pyramidal neurons from young rats: subtypes and gradients. *J Physiol* **525**, 621–639.

Kupper J, Prinz AA & Fromherz P (2002). Recombinant Kv1.3 potassium channels stabilize tonic firing of cultured rat hippocampal neurons. *Eur J Physiol* **443**, 541–547.

Lambe EK & Aghajanian GK (2001). The role of Kv1.2-containing potassium channels in serotonin-induced glutamate release from thalamocortical terminals in rat frontal cortex. *J Neurosci* **21**, 9955–9963.

Lemon N & Turner RW (2000). Conditional spike backpropagation generates burst discharge in a sensory neuron. *J Neurophys* **84**, 1519–1530.

Lipowsky R, Gillessen T & Alzheimer C (1996). Dendritic Na^+ channels amplify EPSPs in hippocampal CA1 pyramidal cells. *J Neurophys* **76**, 2181–2191.

Lisman J (1997). Bursts as a unit of neural information: making unreliable synapses reliable. *Trends Neurosci* **20**, 38–43.

Lopantsev V, Tempel BL & Schwartzkroin PA (2003). Hyperexcitability of CA3 pyramidal cells in mice lacking the potassium channel subunit Kv1.1. *Epilepsia* **44**, 1506–1512.

Magee JC & Carruth M (1999). Dendritic voltage-gated ion channels regulate the action potential firing mode of hippocampal CA1 pyramidal neurons. *J Neurophysiol* **82**, 1895–1901.

Magee JC, Christofi G, Miyakawa H, Christie B, Lasser-Ross N & Johnston D (1995). Subthreshold activation of voltage-gated Ca^{2+} channels mediates a localized Ca^{2+} influx into the dendrites of hippocampal pyramidal neurons. *J Neurophysiol* **74**, 1335–1342.

Magee JC & Johnston D (1995*a*). Characterization of single voltage-gated Na^+ and Ca^{2+} channels in apical dendrites of rat CA1 pyramidal neurons. *J Physiol* **487**, 67–90.

Magee JC & Johnston D (1995*b*). Synaptic activation of voltage-gated channels in the dendrites of hippocampal pyramidal neurons. *Science* **268**, 301–304.

Mainen ZF & Sejnowski TJ (1996). Influence of dendritic structure on firing pattern in model neocortical neurons. *Nature* **32**, 363–366.

Malinow R (1994). LTP: desperately seeking resolution. *Science* **266**, 1195–1196.

Martina M, Schultz JH, Ehmke H, Monyer H & Jonas P (1998). Functional and molecular differences between voltage-gated K^+ channels of fast-spiking interneurons and pyramidal neurons of rat hippocampus. *J Neurosci* **18**, 8222–8125.

Martina M, Yao GL & Bean BP (2003). Properties and functional role of voltage-dependent potassium channels in dendrites of rat cerebellar Purkinje neurons. *J Neurosci* **23**, 5698–5707.

McKay BE, Molineux ML, Mehaffey WH & Turner RW (2005). Kv1 K^+ channels control Purkinje cell output to facilitate postsynaptic rebound discharge in deep cerebellar neurons. *J Neurosci* **25**, 1481–1492.

Metz AE, Jarsky T, Martina M & Spruston N (2005). R-type calcium channels contribute to afterdepolarization and bursting in hippocampal CA1 pyramidal neurons. *J Neurosci* **25**, 5763–5773.

Monaghan MM, Trimmer JS & Rhodes KJ (2001). Experimental localization of Kv1 family voltage-gated K^+ channel α and β subunits in rat hippocampal formation. *J Neurosci* **21**, 5973–5983.

Muller RU, Kubie JL & Ranck JBJ (1987). Spatial firing patterns of hippocampal complex-spike cells in a fixed environment. *J Neurosci* **7**, 1935–1950.

Nisenbaum ES, Wilson CJ, Foehring RC & Surmeier DJ (1996). Isolation and characterization of persistent potassium current in neostriatal neurons. *J Neurophysiol* **76**, 1180–1194.

O'Keefe J (1976). Place units in the hippocampus of the freely moving rat. *Exp Neurol* **51**, 78–109.

Otto T, Eichenbaum H, Wiener SI & Wible CG (1991). Learning-related patterns of CA1 spike trains parallel stimulation parameters optimal for inducing hippocampal long-term potentiation. *Hippocampus* **1**, 181–192.

Pike FG, Meredith RM, Olding AWA & Paulsen O (1999). Postsynaptic bursting is essential for 'Hebbian' induction of associative long-term potentiation at excitatory synapses in rat hippocampus. *J Physiol* **518**, 571–576.

Raab-Graham KF, Haddick PC, Jan YN & Jan LY (2006). Activity- and mTOR-dependent suppression of Kv1.1 channel mRNA translation in dendrites. *Science* **314**, 144–148.

Ranck JBJ (1973). Studies on single neurons in dorsal hippocampal formation and septum in unrestrained rats: Part I: behavioral correlates and firing repertoires. *Exp Neurol* **41**, 461–555.

Rhodes KJ, Strassle BW, Monaghan MM, Bekele-Arcuri Z, Matos MF & Trimmer JS (1997). Association and colocalization of the Kvβ1 and Kvβ3 β-subunits with Kv1 α-subunits in mammalian brain K^+ channel complexes. *J Neurosci* **17**, 8246–8258.

Rothman JS & Manis PB (2003). The roles potassium currents play in regulating electrical activity of ventral cochlear nucleus neurons. *J Neurophysiol* **89**, 3097–3223.

Sah P & Bekkers JM (1996). Apical dendritic location of slow afterhyperpolarization current in hippocampal pyramidal neurons: implications for the integration of long-term potentiation. *J Neurosci* **16**, 4537–4542.

Sanabria ERG, Su H & Yaari Y (2001). Initiation of network bursts by Ca^{2+}-dependent intrinsic bursting in the rat pilocarpine model of temporal lobe epilepsy. *J Physiol* **532**, 205–216.

Schwartzkroin PA (1975). Characteristics of CA1 neurons recorded intracellularly in the hippocampal *in vitro* slice preparation. *Brain Res* **85**, 423–436.

Sheng M, Tsaur ML, Jan YN & Jan LY (1994). Contrasting subcellular localization of the $K_v1.2$ K^+ channel in different neurons of rat brain. *J Neurosci* **14**, 2408–2417.

Southan AP & Robertson B (1998). Patch-clamp recordings from cerebellar basket cells bodies and their presynaptic terminals reveal an asymmetric distribution of voltage-gated potassium channels. *J Neurosci* **1893**, 948–955.

Southan AP & Robertson B (2000). Electrophysiological characterization of voltage-gated K^+ currents in cerebellar basket and Purkinje cells: Kv1 and Kv3 channel subfamilies are present in basket cell terminals. *J Neurosci* **20**, 114–122.

Staff NP, Jung HY, Thiagarajan T, Yao M & Spruston N (2000). Resting and active properties of pyramidal neurons in subiculum and CA1 of rat hippocampus. *J Neurophysiol* **84**, 2398–2408.

Storm JF (1987). Action potential repolarization and a fast after-hyperpolarization in rat hippocampal pyramidal cells. *J Physiol* **385**, 733–759.

Storm JF (1988). Temporal integration by a slowly inactivating K^+ current in hippocampal neurons. *Nature* **336**, 379–381.

Storm JF (1990). Potassium currents in hippocampal pyramidal cells. *Prog Brain Res* **83**, 161–187.

Stühmer W, Ruppersberg JP, Schroter KH, Sakmann B, Stocker M, Giese KP, Perschke A, Baumann A & Pongs O (1989). Molecular basis of functional diversity of voltage-gated channels in mammalian brain. *EMBO J* **8**, 3235–3244.

Su H, Alroy G, Kirson ED & Yaari Y (2001). Extracellular calcium modulates persistent sodium current-dependent burst-firing in hippocampal pyramidal neurons. *J Neurosci* **21**, 4173–4182.

Su S, Sochivko D, Becker A, Chen J, Jiang Y, Yaari Y & Beck H (2002). Upregulation of a T-type Ca^{2+} channel causes a long-lasting modification of neuronal firing mode after status epilepticus. *J Neurosci* **22**, 3645–3655.

Suzuki SS & Smith GK (1985*a*). Single-cell activity and synchronous bursting in the rat hippocampus during waking behavior and sleep. *Exp Neurol* **89**, 71–89.

Suzuki SS & Smith GK (1985*b*). Burst characteristics of hippocampal complex spike cells in the awake rat. *Exp Neurol* **89**, 90–95.

Takigawa T & Alzheimer C (1999). G protein-activated inwardly rectifying K^+ (GIRK) currents in dendrites of rat neocortical pyramidal cells. *J Physiol* **517**, 385–390.

Thomas MJ, Watabe AM, Moody TD, Makhinson M & O'Dell TJ (1998). Postsynaptic complex spike bursting enables the induction of LTP by theta frequency synaptic stimulation. *J Neurosci* **18**, 7118–7128.

Williams SR & Stuart GJ (1999). Mechanisms and consequences of action potential burst firing in rat neocortical pyramidal neurons. *J Physiol* **521**, 467–482.

Wu R & Barish ME (1999). Modulation of a slowly inactivating potassium current, I_D, by metabotropic glutamate receptor activation in cultured hippocampal pyramidal neurons. *J Neurosci* **19**, 6825–6837.

Yasuda R, Sabatini BL & Svoboda K (2003). Plasticity of calcium channels in dendritic spines. *Nat Neurosci* **6**, 948–955.

Yue C, Remy S, Su H, Beck H & Yaari Y (2005). Proximal persistent Na^+ channels drive spike afterdepolarizations and associated bursting in adult CA1 pyramidal cells. *J Neurosci* **25**, 9704–9720.

Yue C & Yaari Y (2004). KCNQ/M channels control spike afterdepolarization and burst generation in hippocampal neurons. *J Neurosci* **24**, 4614–4624.

Yue C & Yaari Y (2006). Axo-somatic and apical dendritic Kv7/M channels differentially regulate the intrinsic excitability of adult rat CA1 pyramidal cells. *J Neurophysiol* **95**, 3480–3495.

Zhang CL, Messing A & Chiu SY (1999). Specific alteration of spontaneous GABAergic inhibition in cerebellar Purkinje cells in mice lacking potassium channel Kv1.1. *J Neurosci* **19**, 2852–2864.

Acknowledgements

The authors are deeply grateful to Dr Bruce Bean for his contribution to the development of the idea of the electronic excision of the dendrite. This work was supported by departmental funds (M.M.) and by NIH grants to N.S. (NS-35180, MH-074866, and RR-015497). A.E.M. was supported by a National Research Service Award from the National Institutes of Health (NS044688).

Supplemental material

Online supplemental material for this paper can be accessed at:
http://jp.physoc.org/cgi/content/full/jphysiol.2006.127068/DC1
and
http://www.blackwell-synergy.com/doi/suppl/10.1113/jphysiol.2006.127068

Dendritic D-type potassium currents inhibit the spike afterdepolarization in rat hippocampal CA1 pyramidal neurons

Alexia E. Metz, Nelson Spruston and Marco Martina

J. Physiol. 2007;581;175-187; originally published online Feb 22, 2007;

DOI: 10.1113/jphysiol.2006.127068